

Dilepton photoproduction measures the fluctuations of initial electromagnetic fields in nuclear collisions

Guansong Li,¹ Kai Zhou,² and Baoyi Chen^{1,3,*}

¹*Department of Physics, Tianjin University, Tianjin 300350, China*

²*Frankfurt Institute for Advanced Studies, Ruth-Moufang-Strae 1, D-60438 Frankfurt am Main, Germany*

³*Institut für Theoretische Physik, Goethe-Universität Frankfurt, Max-von-Laue-Str. 1, D-60438 Frankfurt am Main, Germany*

(Dated: February 2, 2022)

Dilepton production from two photon interactions $\gamma\gamma \rightarrow l^+l^-$ are studied in semi-central and peripheral nuclear collisions. Based on Weizsäcker-Williams approach, It is shown that the dilepton photoproduction is proportional to the electromagnetic (EM) fields $\sim E^2B^2$ and therefore sensitive to the magnitude and lifetime of initial EM fields which last only for a short time and are hard to be measured in experiments directly. We propose dilepton photoproduction as a probe for the nuclear charge fluctuations, which are crucial for the electric/magnetic field induced chiral and charge particle evolutions. We calculate the relative standard deviation of dilepton mass spectrum with event-by-event fluctuating nuclear charge distributions (and EM fields).

In relativistic heavy ion collisions, one of the main goals is to study the properties of the deconfined matter, called “Quark-Gluon Plasma” (QGP) produced in the hadronic collisions of two nuclei [1–3]. In QGP, huge number of light partons are excited and increase the energy density of hot medium in the colliding area. They expand outward violently due to the large spatial gradient of the pressure [4]. The evolutions of light partons with electric charge and chirality are believed to be controlled by the strong interactions. In another aspect, nuclei with electric charges Ze (e is the electron charge) are accelerated to nearly the speed of light, and generate extremely strong electromagnetic (EM) fields with a short lifetime $\sim 2R_A/\gamma_L$ [5, 6], where R_A and γ_L are the nuclear radius and the Lorentz factor of fast moving nucleons. Besides nuclear hadronic collisions, these EM fields can also interact with the target nucleus (moving in the opposite direction) [7–10] or the other EM fields generated by the target nucleus [11–16]. These reactions have been extensively studied in the Ultra-peripheral collisions (UPCs) absent of hadronic collisions [14, 17–21]. The EM fields can reach its maximum value at the order of $eB \sim 10m_\pi^2$ [5] in the semi-central and peripheral collisions with the impact parameter around $b \sim 10$ fm at the colliding energies of Relativistic Heavy Ion Collider (RHIC) and Large Hadron Collider (LHC).

In the semi-central collisions with the existence of both deconfined medium and strong EM fields, the EM fields can affect the evolutions of charge and chiral partons in the early stage of the hot medium expansion, such as Chiral-Magnetic-Effect (CME) [22] and Electric-Separation-Effect (CSE) [23]. However, with the background of strong collective expansions driven by the pressure gradient, electric/magnetic field induced parton evolutions are contaminated and difficult to be quantified

with the final hadron spectra [24, 25]. The signals of these effects in heavy ion collisions are still under debate. Whether these effects are observable or not depends sensitively on the magnitude and lifetime of the initial electromagnetic fields. These EM fields last for a very short time and seems impossible to be measured directly. In this article, we propose that the dilepton photoproduction which is proportional to the $\propto B^4$ (or E^4) can reveal properties of EM fields in the early stage of nuclear collisions [8].

Initial electromagnetic fields can affect chiral/charged particle evolutions, and also produce vector mesons (J/ψ , ϕ , *et al*) and dileptons (e^+e^- , $\mu^+\mu^-$), which have been widely studied in UPCs and is in good agreement with the lowest order Quantum Electrodynamics calculations. In semi-central nuclear collisions of RHIC and LHC energies, experiments have observed the significant yield enhancement of dileptons at the invariant mass of J/ψ , with the feature only in extremely low transverse momentum $p_T < 0.3$ GeV/c [9]. This enhancement is far above the hadronic contributions, and is attributed to the coherent photon-nuclear interactions: EM fields are approximated as quasi-real photons (Weizsäcker-Williams Method) [26, 27] which scatter with the target nucleus moving in the opposite direction and fluctuate into vector mesons.

At the RHIC Au-Au and U-U collisions, experiments also observe a continuum enhancement of e^+e^- in the low invariant mass spectrum $0.4 \text{ GeV} < M_{ll} < 2.6 \text{ GeV}$ with the limitation of $p_T < 0.15 \text{ GeV/c}$ at the impact parameter $b \sim 10$ fm in their preliminary results [28]. The STAR continuum observables are compatible with the two-photon production contribution. This indicates that dilepton photoproduction dominates the yield in the low invariant mass region even in hadronic collisions [15]. In this work, we study the dilepton photoproduction with the fluctuating nuclear charge distributions, which is considered as an important input for the particle evolutions induced by EM fields.

*Email: baoyi.chen@tju.edu.cn

With large Lorentz factor $\gamma_L \sim \sqrt{s_{NN}}/(2m_N)$ where m_N and $\sqrt{s_{NN}}$ are the nucleon mass and the colliding energy, the transverse electric fields of the fast moving nucleus are enhanced by the Lorentz factor, $E_T^i = \gamma_L E_T^{i-RF}$. And their magnitude is similar with the magnetic fields, $|E_T^i| \approx |B_T^i|$ ($i = \text{nucleus 1 or 2}$). Here E_T^{i-RF} is the electric fields in the nuclear rest frame. Meanwhile, the longitudinal component is correspondingly suppressed and therefore negligible. These transverse electromagnetic fields can be approximated to be a swarm of quasi-real photons moving longitudinally [29]. The configuration of EM fields depends on the form factor, which is the Fourier transform of the nuclear charge density,

$$F(\mathbf{q}) = \int \rho_{Au}(\mathbf{r}) \exp(i\mathbf{q} \cdot \mathbf{r}) d\mathbf{r} \quad (1)$$

where $\rho_{Au}(\mathbf{r})$ is the normalized nucleon distribution of Au, $\int d\mathbf{r} \rho_{Au}(\mathbf{r}) = 1$. The photon spectrum is determined by the conservation of energy flux through the transverse plane, $\int dtd\mathbf{x}_T |\mathbf{E}_T \times \mathbf{B}_T| = \int dw d\mathbf{x}_T w n(w, \mathbf{x}_T)$, and then the photon density is

$$\frac{dN_\gamma}{dw d\mathbf{x}_T} = \frac{Z^2 \alpha}{4\pi^3 w} \left| \int_0^\infty dk_T k_T^2 \frac{F(\mathbf{k}_T^2 + (\frac{w}{\gamma_L})^2)}{\mathbf{k}_T^2 + (\frac{w}{\gamma_L})^2} J_1(x_T k_T) \right|^2 \quad (2)$$

with $\alpha = e^2/(\hbar c) = (4\pi)/137$. w and k_T is the photon energy and transverse momentum respectively. J_1 is the first kind Bessel function. In the collisions with $b < 2R_A$, protons in the overlap area are suddenly decelerated by hadronic collisions, and do not contribute to the dilepton photoproduction, see the schematic diagram below [13]. In this work, we focus on the effects of nuclear charge fluctuations on dilepton photoproduction. As a comparison, the smooth case is also studied where the nucleon density is taken to be the smooth Woods-Saxon distribution,

$$\rho_{Au}(\mathbf{r}) = \frac{\rho_0}{1 + \exp(\frac{r-r_0}{a})} \quad (3)$$

with $\rho_0 = \frac{1}{A_{Au}} 0.1694 \text{ fm}^{-3}$, $r_0 = 6.38 \text{ fm}$ and $a = 0.535 \text{ fm}$. For the fluctuating distributions of electric charges (or protons) in the nucleus, we generate each proton position with Eq.(3) by Monte Carlo simulations in each colliding event [5]. The protons in the nucleus are not taken as point charge, instead, they are treated with a finite size to avoid the singularities in EM fields and the photon spatial densities. Eq.(3) is also employed for charge distribution in proton with different parameters,

$$\rho_p(\mathbf{r}) = \frac{\rho_{p0}}{1 + \exp(\frac{r-r_{p0}}{a_p})} \quad (4)$$

where the origin of coordinate is put at the center of the proton. $r_{p0} = 1.2 \text{ fm}$ and $a_p = a$ describe the size and shape of a proton. $\rho_{p0} = 0.0458 \text{ fm}^{-3}$ is fixed by the normalization of Eq.(4) to be unit.

After randomly generating proton positions in the nucleus, the fluctuating charge densities in the nucleus can be written as

$$\rho_{\text{fluct}}(\mathbf{r}) = \sum_{i=1}^Z \rho_p(\mathbf{r} - \mathbf{r}_i) \quad (5)$$

where \mathbf{r}_i is the position of each proton relative to the nuclear center. Note that the smooth disposal of proton charges slightly extend the nuclear charge distribution to the nuclear surface compared with Woods-Saxon distribution, cf. black solid line in Fig.1. The dilepton yield will be a little different when employing the averaged and Woods-Saxon nuclear charge distributions. On the other hand, the standard deviation of dilepton photoproduction is less affected, and mainly attributed to the fluctuations of charge densities in each colliding events.

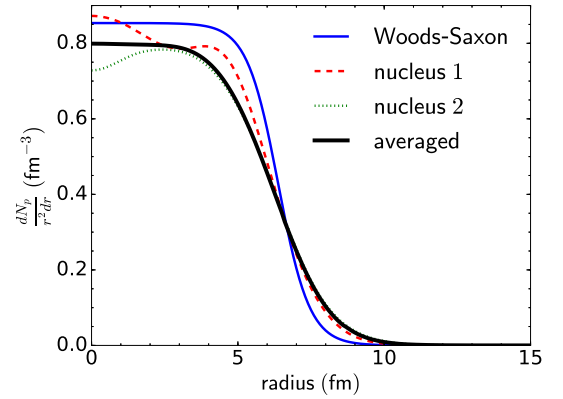


FIG. 1: (Color Online) Nuclear charge fluctuations in event-by-event MC simulations. The fluctuating electric charge densities in *nucleus 1* and *nucleus 2* are independent from each other, and deviate from the averaged distribution.

With photon density $n(w, \mathbf{x}_T) \equiv dN_\gamma/(dw d\mathbf{x}_T)$ at the transverse coordinate $\mathbf{x}_T = \mathbf{r} = (x, y)$, we can calculate the dilepton production from two-photon scatterings, $\gamma\gamma \rightarrow l\bar{l}$. In this work, we neglect the contribution of electric charges in the area of hadronic collisions, and only consider the EM fields generated by spectator protons. The EM fields from spectator protons spread over the entire transverse plane, which makes quasi-real photons also distribute over the entire transverse plane including the area inside the nucleus and hadronic collision zone. Therefore, the spatial integration of $\gamma\gamma \rightarrow l\bar{l}$ is over the entire transverse plane, see Eq.(6) and Fig.2. Now we write the dilepton photoproduction in AA collisions with the impact parameter $b < 2R_A$ as below,

$$\frac{dN}{dM_{l\bar{l}}} = \int_{-\infty}^{+\infty} dY \int_0^{2\pi} d\theta \int_0^{+\infty} r dr n_1(w_1, r_1) n_2(w_2, r_2) \sigma_{\gamma\gamma \rightarrow l\bar{l}} \frac{M_{\gamma\gamma}}{2} \quad (6)$$

where $Y = 1/2 \ln(w_1/w_2)$ and $M_{l\bar{l}} = 2\sqrt{w_1 w_2}$ are determined by the energies of two scattering photons w_1 and

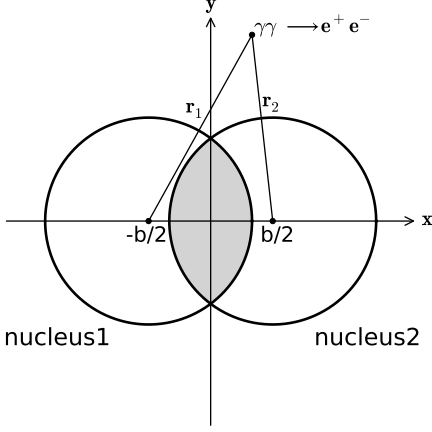


FIG. 2: Schematic diagram for two-photon scatterings $\gamma\gamma \rightarrow f\bar{f}$ (f is fermion) in the relativistic collisions between nucleus 1 and 2. b is the impact parameter. The electric charges in the overlap area do not contribute to the two-photon scatterings. The origin of coordinates is set in the middle of two nuclear centers.

w_2 . The distance between the scattering position and two nuclear centers are $r_1 = \sqrt{b^2/4 + r^2 - 2br \cos \theta}$ and $r_2 = \sqrt{b^2/4 + r^2 + 2br \cos \theta}$ respectively, and r is the coordinate of the scattering in Fig.2. The cross section of two-photon scattering is extracted by the Breit-Wheeler formula [30],

$$\sigma_{\gamma\gamma \rightarrow l\bar{l}} = \frac{4\pi\alpha^2}{M_{l\bar{l}}^2} \left[\left(2 + \frac{8m^2}{M_{l\bar{l}}^2} - \frac{16m^4}{M_{l\bar{l}}^4} \right) \ln \left(\frac{M_{l\bar{l}} + \sqrt{M_{l\bar{l}}^2 - 4m^2}}{2m} \right) - \sqrt{1 - \frac{4m^2}{M_{l\bar{l}}^2}} \left(1 + \frac{4m^2}{M_{l\bar{l}}^2} \right) \right] \quad (7)$$

where m is the lepton mass and $M_{l\bar{l}}$ is the invariant mass of dilepton.

Before studying the dilepton photoproduction with fluctuating EM fields, we consider the situation of smooth charge distribution. In Fig.3, we calculate the e^+e^- invariant mass spectrum $dN/dM_{e^+e^-}$ at the impact parameter $b = 10$ fm and 15 fm in $\sqrt{s_{NN}} = 200$ GeV Au-Au collisions. In peripheral collisions without hadronic collisions, dilepton production only come from the interactions of EM fields generated by two nuclei. In the situation with $b = 10$ fm, final dilepton yields consist of photoproduction from two-photon scatterings and thermal emission from QGP. In the low invariant mass spectrum, dilepton production is dominated by the photoproduction, and we neglect the contribution of QGP which is the main source at larger invariant mass region. In semi-central collisions, we exclude the contribution of electric charges inside the overlap of two nuclei [13, 15]. Considering that realistic nuclear charge distribution is continuous, and EM fields inside the nucleus is non-zero, the photon spatial density inside the nucleus is also non-zero

and contributes to the dilepton photoproduction in our calculations.

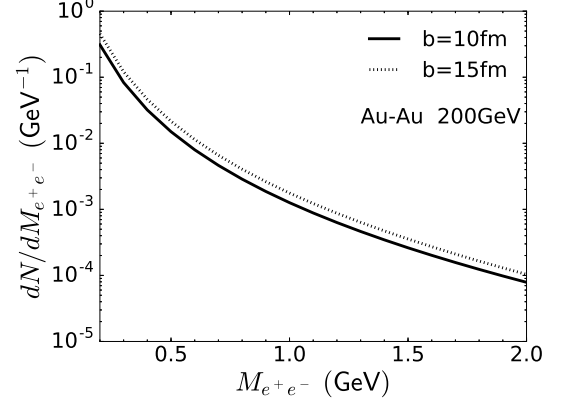


FIG. 3: Invariant mass spectra of photoproduced e^+e^- at the impact parameter $b = 10$ fm (dashed line) and $b = 15$ fm (dotted line) with the Woods-Saxon distribution. Note that dilepton production with $M_{e^+e^-} > 0.4$ GeV is measurable in STAR Collaboration.

Now, we take the fluctuating charge distribution $\rho_{\text{fluct}}(\mathbf{r})$ to calculate the photon densities and the dilepton photoproduction. The fluctuations of proton positions in the transverse plane is random, which make nuclear charge distribution non-isotropic anymore. In order to simplify the numerical calculations of photon density with Eq.(2), we only consider the radial fluctuations in ρ_{fluct} and employ the fluctuating isotropic nuclear charge density (cf. Fig.1) in the following calculations. With different charge distributions in each event of Au-Au collisions, the strength of EM fields is different. If the protons are distributed in the area of hadronic collisions due to the fluctuations, they will not contribute to the dilepton photoproduction, and Z_{eff} of this event will be smaller than its mean value. We can obtain the fluctuations of dilepton production induced by the nuclear charge fluctuations. Considering that particle yield is a scalar observable, the average of dilepton yields over many events will partially eliminate the effects of fluctuations. Therefore, we evaluate the relative standard deviation of dilepton production, $\frac{\sqrt{\langle (X - \langle X \rangle)^2 \rangle}}{\langle X \rangle}$. Here $X \equiv dN/dM_{e^+e^-}$ is the dilepton production in one configuration of fluctuating EM fields, and $\langle X \rangle$ is the averaged yield over many events. This observable is weakly affected by the uncertainties of two-photon scattering cross sections $\sigma_{\gamma\gamma \rightarrow l\bar{l}}$ and is mainly attributed to the fluctuations of photon densities (EM fields). The ratio is around $(4 \sim 5)\%$ in the experimentally measurable region of invariant mass $0.4 < M_{e^+e^-} < 2$ GeV, cf. Fig.4.

In summary, we calculate the dilepton photoproduction from electromagnetic fields in peripheral and semi-central collisions. In the low invariant mass region and close-to-peripheral collisions, dilepton yields from hot medium radiation produced in the nuclear hadronic collisions are relatively small compared with the photopro-

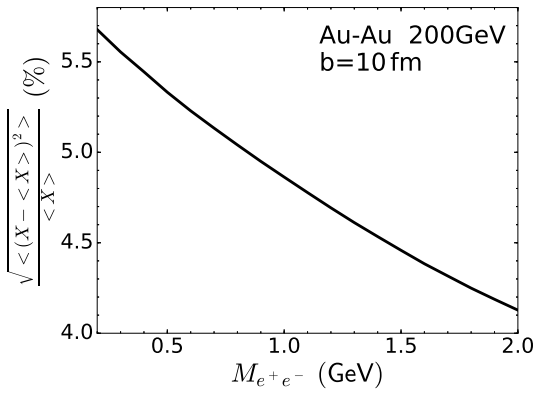


FIG. 4: Relative standard deviation $\frac{\sqrt{\langle (X - \langle X \rangle)^2 \rangle}}{\langle X \rangle}$ for dilepton photoproduction with event-by-event fluctuating EM fields as a function of invariant mass. $X \equiv dN/dM_{e^+e^-}$ is the dilepton spectrum.

duction. We simulate the fluctuations of proton positions in the nucleus, which results in event-by-event fluctuating electromagnetic fields. We calculate the dilepton photoproduction based on fluctuating EM fields, and show the relative standard deviation $\frac{\sqrt{\langle (X - \langle X \rangle)^2 \rangle}}{\langle X \rangle}$ of their yields $X \equiv dN/dM_{l\bar{l}}$. It is less affected by the dilepton cross section $\gamma\gamma \rightarrow l\bar{l}$, and mainly depends on the spatial configurations of quasi-real photons (or EM fields), which can help revealing the fluctuations of initial EM fields in the nuclear collisions. In the next step, we will focus on the polarization of photoproduced particles, which is more sensitive to the combined EM fields of two nuclei and their fluctuations.

Acknowledgement: BC acknowledges helpful discussions with Enrico Speranza. This work is supported by NSFC Grant No. 11705125, 11547043 and Sino-Germany (CSC-DAAD) Postdoc Scholarship. KZ kindly acknowledge support by the AI grant of SAMSON AG, Frankfurt.

-
- [1] M. Gyulassy and L. McLerran, Nucl. Phys. A **750**, 30 (2005)
 - [2] E. V. Shuryak, Nucl. Phys. A **750**, 64 (2005)
 - [3] H. Song, S. A. Bass, U. Heinz, T. Hirano and C. Shen, Phys. Rev. Lett. **106**, 192301 (2011) Erratum: [Phys. Rev. Lett. **109**, 139904 (2012)]
 - [4] H. Song and U. W. Heinz, Phys. Rev. C **78**, 024902 (2008)
 - [5] W. T. Deng and X. G. Huang, Phys. Rev. C **85**, 044907 (2012)
 - [6] K. Tuchin, Adv. High Energy Phys. **2013**, 490495 (2013)
 - [7] S. Klein and J. Nystrand, Phys. Rev. C **60**, 014903 (1999)
 - [8] W. Shi, W. Zha and B. Chen, Phys. Lett. B **777**, 399 (2018)
 - [9] J. Adam *et al.* [ALICE Collaboration], Phys. Rev. Lett. **116** (2016) no.22, 222301
 - [10] V. Khachatryan *et al.* [CMS Collaboration], Phys. Lett. B **772**, 489 (2017)
 - [11] J. Adams *et al.* [STAR Collaboration], Phys. Rev. C **70**, 031902 (2004)
 - [12] G. Baur, K. Hencken, D. Trautmann, S. Sadovsky and Y. Kharlov, Phys. Rept. **364**, 359 (2002)
 - [13] A. J. Baltz, Y. Gorbunov, S. R. Klein and J. Nystrand, Phys. Rev. C **80**, 044902 (2009)
 - [14] M. Aaboud *et al.* [ATLAS Collaboration], Nature Phys. **13**, no. 9, 852 (2017)
 - [15] W. Zha, L. Ruan, Z. Tang, Z. Xu and S. Yang, Phys. Lett. B **781**, 182 (2018)
 - [16] S. R. Klein, Phys. Rev. C **97**, no. 5, 054903 (2018)
 - [17] A. J. Baltz *et al.*, Phys. Rept. **458**, 1 (2008)
 - [18] G. M. Yu and Y. D. Li, Phys. Rev. C **91**, no. 4, 044908 (2015); G. M. Yu, G. G. Zhao, Z. Bai, Y. B. Cai, H. T. Yang and J. S. Wang, Adv. High Energy Phys. **2017**, 2379319 (2017); G. M. Yu, Y. C. Yu, Y. D. Li and J. S. Wang, Nucl. Phys. B **917**, 234 (2017)
 - [19] G. Baur, K. Hencken and D. Trautmann, Phys. Rept. **453**, 1 (2007)
 - [20] S. R. Klein, J. Nystrand, J. Seger, Y. Gorbunov and J. Butterworth, Comput. Phys. Commun. **212**, 258 (2017)
 - [21] E. Abbas *et al.* [ALICE Collaboration], Eur. Phys. J. C **73**, no. 11, 2617 (2013)
 - [22] D. E. Kharzeev, L. D. McLerran and H. J. Warringa, Nucl. Phys. A **803**, 227 (2008)
 - [23] X. G. Huang and J. Liao, Phys. Rev. Lett. **110**, no. 23, 232302 (2013)
 - [24] S. Shi, Y. Jiang, E. Lilleskov and J. Liao, Annals Phys. **394**, 50 (2018)
 - [25] H. j. Xu, J. Zhao, X. Wang, H. Li, Z. W. Lin, C. Shen and F. Wang, arXiv:1710.07265 [nucl-th].
 - [26] E. J. Williams, Proc. Roy. Soc. A **139**, 163 (1933)
 - [27] C. F. von Weizsacker, Z. Phys. **88**, 612 (1934)
 - [28] J. D. Brandenburg [STAR Collaboration], Nucl. Phys. A **967**, 676 (2017)
 - [29] F. Krauss, M. Greiner and G. Soff, Prog. Part. Nucl. Phys. **39**, 503 (1997).
 - [30] S. J. Brodsky, T. Kinoshita and H. Terazawa, Phys. Rev. D **4**, 1532 (1971).